Magnetic and electric properties of the Hubbard model for the fcc lattice

D. Grensing, E. Marsch,* and W. -H. Steeb
Institut für Theoretische Physik der Universität Kiel D-23 Kiel, West Germany

(Received 22 August 1977)

Using the Hartree-Fock approximation, the half-filled Hubbard model is investigated for the fcc lattice at absolute zero. The results are quite different from those obtained for the simple cubic lattice arising from the nonsymmetric band structure of the nonalternate lattice. It is found that antiferromagnetism appears only when the intra-atomic Coulomb interaction U exceeds a critical value. This magnetic phase transition from a paramagnetic to an antiferromagnetically ordered phase proves to be of first order. With increasing U, a metal-insulator transition occurs, caused by band separation. The gap collapse at the first critical U causes jumps in the curves of conductivity and spin susceptibility. Both quantities are calculated as functions of U with the aid of a generalized density of states. Investigating criteria for the onset of magnetism and constructing a magnetic phase diagram for variable band occupation, the antiferromagnetic state is found to be stable with respect to ferromagnetic ordering in the region of finite U only for electron densities within $0.27 < n_e < 1.21$. In the strong coupling limit $U \to \infty$ this stability criterion must be modified and is shown to coincide with the predictions of Nagaoka's rigorous investigations of an almost half-filled band. In the case where the band is almost filled, a first-order paramagnetic to ferromagnetic transition is obtained at a finite value of U, whereas the critical curve defining the antiferromagnetic phase boundary diverges as n_e approaches $n_e = 2$. For a band which is almost vacant, the competitive phase boundaries both yield unphysically large values of U. In the latter case there is no magnetic phase transition in a region of experimentally observable values of U at all.

I. INTRODUCTION

Theoretical analysis of the Hubbard Hamiltonian for the case of a half-filled band has been concerned with the possible existence of an insulator to metal transition.[1-3] In particular the Hartree-Fock approximation[4-10] (HFA) has been used to investigate this question. However, in most of the works only alternate lattices are considered. These are lattices which can support a simple AB sublattice structure where all nearest neighbors of the A sites belong to the B sublattice and vice versa. Examples for such lattices are the linear chain, the two-dimensional square lattice, the simple cubic (sc) and bcc lattice. Moreover in all works only nearest-neighbor (NN) hopping is taken into account. It has been found that in this case of AB lattice and NN hopping the condition for antiferromagnetism in the HFA is isomorphic to the gap equation of the superconductivity theory. Thus all alternate lattices, with NN hopping only, exhibit insulating antiferromagnetism for any nonvanishing U, where U denotes the value of the interaction strength. Note that this result is consistent with the exact solution of the model[11] for the linear chain. The reason for this behavior has been widely discussed by Penn[5] and Brandow.[12] The point is that there exists a wave vector $\vec{Q}$ characterizing the extra periodicity due to the antiferromagnetic ordering. $\vec{Q}$ is defined by the condition that $\exp(i\vec{Q}\cdot\vec{t}) = -1$ for all translations t which transform one sublattice into the other. For the sc lattice one has $\vec{Q} = \pi(1,1,1)$ and therefore the band energies satisfy the perfect nesting condition $\epsilon(\vec{k}+\vec{Q}) = -\epsilon(\vec{k})$. Recently, it has been shown[13] that for the linear chain, where nearest- and next-nearest-neighbor (NNN) hopping is taken into account, new results arise when the hopping strength to the next-nearest neighbors exceeds a critical value. In this case a phase transition from a paramagnetic to an antiferromagnetic state occurs, which proves to be of first order and is combined with a collapse in the energy gap. Moreover, a metal-insulator transition is found which, however, occurs at a smaller value of U and lies in a region of phase coexistence. These phenomena of a gap collapse and the separation of the magnetic and electric phase transitions are due to the nonsymmetric band energies and the corresponding density of states. Thus we expect that investigations of the linear chain with nearest- and next-nearest-neighbor hopping already anticipate general features of nonalternate lattices.

In this paper we study the ground state of the Hubbard model within the HFA for the fcc lattice, a typical representative of non-AB lattices. At absolute zero, on increasing U we find the successive phases: (i) nonmagnetic metal, (ii) antiferromagnetic (AFM) metal, and (iii) AFM insulator. Due to the nonsymmetric band structure, the perfect nesting condition no longer holds. Thus one expects, as for the linear chain with NNN hopping, the AFM order to set in at a nonzero Coulomb interaction U and the metal-insulator transition to be separated distinctly from this magnetic transition. It should be emphasized that the chemical potential is no longer given by $\mu=\frac{1}{2}U$ as in the case for the alternate lattice, and must be determined by a self-consistent equation.

In Sec. II the magnetic structure and the appropriate $\vec{Q}$ are determined. This means factorizing the Hamiltonian to obtain a one-particle operator. With the aid of the Green's-function technique, the ground-state energy, chemical potential, gap equation, magnetization, conductivity, and electron susceptibility are evaluated in Sec. III. Following this, the general features of a combined electronic density of states, defined for numerical purpose in the AFM phase, are discussed.

Section IV is devoted to the numerical treatment and the discussion of the results. In particular, since phase transitions of first and second order occur, the stability of the solutions has to be examined, finally resulting in a phase diagram for all possible values of the electron density n_e.

II. DETERMINATION OF THE MAGNETIC CONFIGURATION

In this section we set up the Gorkov equations for the electron Green's functions of a system described by the grand canonical Hubbard Hamiltonian with an applied external field ζ,

$$H=\sum_{\vec{k}\sigma}[\epsilon(\vec{k})-\mu-\zeta\,\mathrm{sgn}(\sigma)]c^{\dagger}_{\vec{k}\sigma}c_{\vec{k}\sigma} + UN^{-1}\sum_{\vec{k}}\sum_{\vec{q}} c^{\dagger}_{\vec{k}+\vec{q}\uparrow}c_{\vec{k}\uparrow}c^{\dagger}_{\vec{k}'-\vec{q}\downarrow}c_{\vec{k}'\downarrow} \quad . \tag{1}$$

$\epsilon(\vec{k})$ denotes the band energy, and N is the number of lattice sites. Choosing basic vectors in the fcc lattice, which point from a cube corner to the nearest face centers, the band energy assumes the form

$$\epsilon(\vec{k})=-2J[\cos k_x+\cos(k_y-k_z)+\cos k_y+\cos(k_z-k_x)+\cos k_z+\cos(k_x-k_y)] \quad , \tag{2}$$

and the components of the wave number $\vec{k}$ satisfy $-\pi<k_j<\pi$ $(j=x,y,z)$.

The Hamiltonian will be treated in a manner used commonly in the theory of superconductivity. This treatment is equivalent to a Hartree-Fock approximation within Green's-function technique. The interaction operator is approximated in Eq. (1) by a bilinear form, i.e., it is replaced by the one-particle Hamiltonian

$$H_{\mathrm{eff}}=\sum_{\vec{k},\sigma}[\epsilon(\vec{k})-\bar{\mu}-\bar{\zeta}\,\mathrm{sgn}(\sigma)]c^{\dagger}_{\vec{k}\sigma}c_{\vec{k}\sigma} + \sum_{\vec{k},l}(\Delta_l c^{\dagger}_{\vec{k}+\vec{Q}_l\uparrow}c_{\vec{k}\downarrow}+\Delta_l^{*}c^{\dagger}_{\vec{k}\downarrow}c_{\vec{k}+\vec{Q}_l\uparrow}) + \sum_{\vec{k},l,\sigma}\Psi_{l-\sigma}c^{\dagger}_{\vec{k}\sigma}c_{\vec{k}+\vec{Q}_l\sigma}-\tfrac{1}{2}E_0 \quad . \tag{3}$$

This Hamiltonian can serve as well as a test Hamiltonian when using Bogoliubov's variational principle, where the quantities we describe below would act as variational parameters. μ and ζ are no longer the true chemical potential and magnetic field, but are now defined by $\bar{\mu}=\mu-\frac{1}{2}n_eU$ and $\bar{\zeta}=\zeta+Us_z$, respectively. n_e denotes the number of electrons and s_z the z component of spin per atom. The quantities $\Psi_{l\uparrow}$, $\Psi_{l\downarrow}$, Δ_l stand for

$$\Psi_{l\sigma}=UN^{-1}\sum_{\vec{k}}\langle c^{\dagger}_{\vec{k}\sigma}c_{\vec{k}+\vec{Q}_l\sigma}\rangle \quad , \tag{4}$$

$$\Delta_l=UN^{-1}\sum_{\vec{k}}\langle c_{\vec{k}+\vec{Q}_l\uparrow}c^{\dagger}_{\vec{k}\downarrow}\rangle \quad . \tag{5}$$

Here the angular brackets denote an ensemble average with the density operator

$$\exp(-\beta H_{\mathrm{eff}})/\mathrm{Tr}\exp(-\beta H_{\mathrm{eff}}) \quad .$$

Finally since we have counted the potential energy twice in this way, we substract the term $\frac{1}{2}E_0$, where E_0 is one-half of the total ensemble-averaged potential energy.

Thus far, the wave numbers $\vec{Q}_l$ are completely at our disposal. In the sc lattice, this set of vectors reduces to the single one $\vec{Q}=\pi(1,1,1)$ obeying the condition of commensurability, i.e., $\exp(i2\vec{Q}\cdot\vec{n})=1$, where $\vec{n}$ denotes a lattice vector.

In order to specify the set $\{\vec{Q}_l\}$ in the fcc lattice, we require that the elements of this set satisfy the condition of commensurability and, together with the unit element $2\pi(1,1,1)=0$, form a group, ensuring that the corresponding system of equations of motion for the Green's functions becomes closed and solvable. The smallest group of symmetrically built vectors $\vec{Q}_l$ is the set $\vec{Q}_1=\pi(0,1,1)$, $\vec{Q}_2=\pi(1,0,1)$, $\vec{Q}_3=\pi(1,1,0)$. These wave numbers point from a minimum to a maximum of the band energy $\epsilon(\vec{k})$ [a property they share with the corresponding wave number $\vec{Q}=\pi(1,1,1)$ in the sc lattice] and are just the quantities one would fall upon when investigating low-lying excitations.[14] This procedure is quite similar to that carried out in the case of the sc lattice and yielding the vector $\vec{Q}=\pi(1,1,1)$.[9] However, using this set $\{\vec{Q}_1,\vec{Q}_2,\vec{Q}_3\}$, the subsequent program which consists of the solution of the equations of motion for the

Green's functions and the evaluation of the thermodynamic quantities of the system, proves to be too ambitious. Therefore we insist only on the condition of commensurability and reduce the set of vectors $\vec{Q}_l$ to the single vector $\vec{Q}_1$. Thus we try to copy the antiferromagnetic ordering of alternant lattices, the difference being that the band energy no longer satisfies the perfect nesting condition and the magnetization whose Fourier components are Δ, $\Psi_\uparrow$, $\Psi_\downarrow$ no longer exhibits the symmetry of the lattice.

In this situation it seems to be advisable to try a new simplification and to set $\Psi_\sigma = 0$ which is another step towards an impressed *AB* structure that can be seen from the reduced effective Hamiltonian

$$H_{\text{eff}} = \sum_{\vec{k}\sigma} [\epsilon(\vec{k}) - \bar{\mu} - \bar{\zeta}\,\text{sgn}(\sigma)] c^{\dagger}_{\vec{k}\sigma} c_{\vec{k}\sigma} + \sum_{\vec{k}} (\Delta c^{\dagger}_{\vec{k}+\vec{Q}_1\downarrow} c_{\vec{k}\downarrow} + \Delta^* c^{\dagger}_{\vec{k}\downarrow} c_{\vec{k}+\vec{Q}_1\downarrow}) - \tfrac{1}{2} E_0 \quad . \tag{6}$$

Transforming back into the Wannier representation, the interaction term can be written in a more compact way,

$$H_{\text{int}} = \sum_{\vec{n}} \vec{H}(\vec{n}) \cdot \vec{S}(\vec{n}) \quad , \tag{7}$$

where $\vec{H}(\vec{n})$ is the magnetic field

$$\vec{H}(\vec{n}) = 2\Delta(\exp(i\vec{Q}\cdot\vec{n}), 0, 0,)$$

and $\vec{S}(\vec{n})$ denotes the spin operator with the x component

$$\vec{S}(\vec{n})_x = \tfrac{1}{2}(c^{\dagger}_{\vec{n}\uparrow} c_{\vec{n}\downarrow} + c^{\dagger}_{\vec{n}\downarrow} c_{\vec{n}\uparrow}) \quad ,$$

etc. Thus the interaction term of Eq. (7) is the same as the Hamiltonian of a spin-system in a magnetic field shown in Fig. 1. The property and obvious disadvantage of this field is the fact that every lattice point is surrounded by eight next neighbors with an opposite direction and four next neighbors with the same direction of the magnetic field H. This magnetic configuration with four wrong next neighbors is not completely adapted to the symmetry of the lattice. Since a decrease of the number of adjacent parallel spins increases the possibility of hopping and thus lowers the kinetic energy of the system, the chosen configuration obviously is not the energetically most favored one. But this incomplete antiferromagnetic ordering cannot be improved as long as the y and z components of the magnetic field $H(n)$ are assumed to be zero ($\Psi_\uparrow = \Psi_\downarrow = 0$). Nevertheless we do not expect the energy differences of the various antiferromagnetic states to be of such an importance as is the general aspect of magnetic ordering itself.

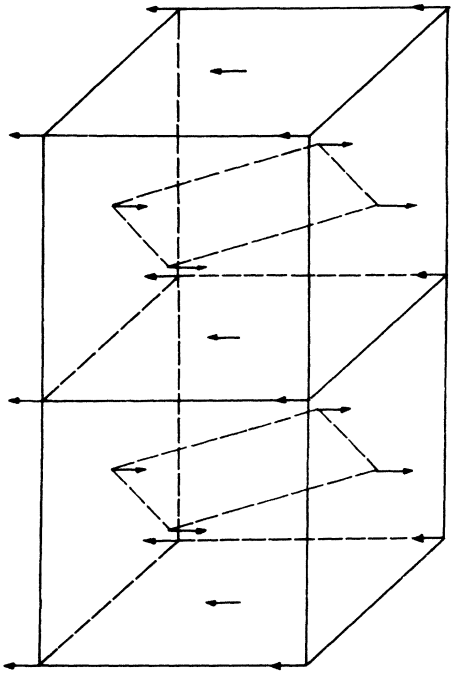

FIG. 1. Magnetic configuration representing the interaction term of the reduced effective Hamiltonian.

III. BASIC HARTREE-FOCK (HF) EQUATIONS

We now use the Green's-function technique[15] and define the Green's function

$$G_{\sigma\sigma'}(\vec{k}, \vec{q}, \tau, \tau') = -\langle T_\tau [c_{\vec{k}\sigma}(\tau) c^{\dagger}_{\vec{k}+\vec{q}\sigma'}(\tau')] \rangle \quad ,$$

where $\vec{q}$ is an element of the set $\{\vec{0}, \vec{Q}_1\}$. T_τ denotes the time-ordering operator and the time-dependent operators are defined as in the Heisenberg picture. As a final step in this procedure we differentiate with respect to τ and introduce the Fourier representation

$$G_{\sigma\sigma'}(\vec{k}, \vec{q}, \tau, \tau') = (\beta\hbar)^{-1} \sum_n G_{\sigma\sigma'}(\vec{k}, \vec{q}, \omega_n) \times \exp[-i\omega_n(\tau - \tau')] \quad ,$$

where the choice $\omega_n = (2n+1)/\beta\hbar$ guarantees the proper Fermi statistics. Then the equations of motion are found to be a pair of simple algebraic equations which must be solved along with the self-consistency conditions

$$\Delta = -UN^{-1} \sum_{\vec{k}} G_{\uparrow\downarrow}(\vec{k}, \vec{Q}_1, \tau - \tau' = 0+) \quad , \tag{8}$$

$$N_\sigma = \sum_{\vec{k}} \langle c^{\dagger}_{\vec{k}\sigma} c_{\vec{k}\sigma} \rangle = \sum_{\vec{k}} G_{\sigma\sigma}(\vec{k}, \vec{0}, \tau - \tau' = 0-) \quad . \tag{9}$$

Substituting the results of the equations of motion into the self-consistency conditions (8) and (9) yields the gap equation and a formula which determines the chemical potential

$$\Delta = \Delta U(2N)^{-1} \sum_{\substack{\vec{k} \\ \nu=1,2}} \frac{(-)^\nu f(E_\nu(\vec{k}))}{E(\vec{k})} \quad , \tag{10}$$

$$N_\sigma = \frac{1}{2}\sum_{\substack{\vec{k}\\ \nu=1,2}} f(E_\nu(\vec{k})) - \frac{\sigma}{2}\sum_{\substack{\vec{k}\\ \nu=1,2}} \frac{(-)^\nu f(E_\nu(\vec{k}))[\epsilon^-(\vec{k})-\bar{\zeta}]}{E(\vec{k})} \quad . \tag{11}$$

$E_\nu(\vec{k})$ are the particle energies

$$E_{1,2}(\vec{k}) = -\bar{\mu} + \epsilon^+(\vec{k}) \pm \{\Delta^2 + [\epsilon^-(\vec{k})-\bar{\zeta}]^2\}^{1/2} \quad , \tag{12}$$

where

$$\epsilon^\pm(\vec{k}) = \tfrac{1}{2}[\epsilon(\vec{k}) \pm \epsilon(\vec{k}+\vec{Q}_1)] \quad ,$$

$E(\vec{k})$ stands for the square-root term in Eq. (12), and f denotes the Fermi function. Utilizing the gap equation, we now perform the integration in the formula for the thermodynamic potential expressed in terms of the interaction Hamiltonian

$$\Omega - \Omega_0 = \int_0^U \frac{d\lambda}{\lambda}\langle \lambda H_{int}\rangle_\lambda \quad , \tag{13}$$

where λ is the coupling strength and Ω_0 is the thermodynamic potential of the noninteracting system. We only quote the result of this well-known procedure:

$$\frac{\Omega}{N} = -\bar{\mu} - U(\tfrac{1}{4}n_e^2 - s_z^2) + \frac{\Delta^2}{U} - (\beta N)^{-1} \times \sum_{\vec{k}\nu} \ln\{2\cosh[\tfrac{1}{2}\beta E_\nu(\vec{k})]\} \quad . \tag{14}$$

It should be noted that for finite temperature Eq. (14) is only physically reasonable in the weak-coupling region.[16] The thermodynamic potential shows an analytic form already known from previous calculations in AB lattices.[6] Thus, at first sight, the nonalternant fcc lattice discussed in this paper, seems to exhibit the same thermodynamic properties in the scope of the performed approximations. But the main difference arises from the nonsymmetric band structure and the quite different behavior of the chemical potential, which will be discussed later. Moreover, the modified band energy $\epsilon^+(\vec{k})$ does not vanish and $\epsilon^-(\vec{k})$ no longer reduces to the original band energy $\epsilon(\vec{k})$. Consequently, we cannot use the usual density of states $g(\epsilon)$ for numerical calculations,[17] but are forced to convert momentum integrals into energy integrals with the help of the combined density of states first introduced by Brandt[10]:

$$g(x,y) = N^{-1}\sum_{\vec{k}} \delta(x-\epsilon^+(\vec{k}))\delta(y-\epsilon^-(\vec{k})) \quad , \tag{15}$$

which we discuss in Appendix A.

The determination of the thermodynamic properties, following from the grand potential of Eq. (14), will be done in a subsequent paper. Here we will investigate only the ground-state energy which can be deduced from Eq. (14) letting $\beta \to \infty$,

$$\frac{E_0}{N} = 2\bar{\zeta}s_z + \bar{\mu}(n_e - 1) + U(\tfrac{1}{4}n_e^2 - s_z^2) + \frac{\Delta^2}{U} - (2N)^{-1}\sum_{\vec{k},\nu}|E_\nu(\vec{k})| \quad . \tag{16}$$

The ground-state energy has to be determined with the help of the self-consistency equations. At absolute zero, these have the simple form

$$1 = -U(4N)^{-1}\sum_{\vec{k},\nu}\frac{(-1)^\nu \operatorname{sgn}[E_\nu(\vec{k})]}{E(\vec{k})} \quad , \tag{17}$$

$$n_e - 1 = -(2N)^{-1}\sum_{\vec{k},\nu}\operatorname{sgn}[E_\nu(\vec{k})] \quad , \tag{18}$$

$$s_z = (4N)^{-1}\sum_{\vec{k},\nu}\frac{(-1)^\nu \operatorname{sgn}[E_\nu(\vec{k})][\epsilon^-(\vec{k})-\bar{\zeta}]}{E(\vec{k})} \quad . \tag{19}$$

We want to emphasize that Eq. (16) is a good approximation over the whole range of the coupling strength U/J for $n_e = 1$. By some simple modifications of the results of Grensing and Koppe[16] one can also show Eqs. (16)–(19) to be valid in the strong-coupling region $U/J \gg 1$. One must certainly admit that this behavior seems to be mathematically singular because finite temperatures and $n_e \neq 1$ lead to a quite different situation as outlined by the above cited authors and in a recent paper of Heise and Jelitto.[18] The gap equation (17) always allows the trivial solution $\Delta = 0$. Demanding that $\Delta = 0$ be the only solution leads to the inequality

$$U^{-1} \leq N^{-1}\sum_{\vec{k}}\frac{\Theta(\epsilon(\vec{k})-\bar{\mu})}{\epsilon^-(\vec{k})} \quad . \tag{20}$$

This condition can also be obtained from an expansion of the ground-state energy in powers of Δ^2 and the requirement that the coefficient of Δ^2 be negative. Both procedures yield the same critical value of U, indicating a second order phase transition into a magnetically ordered phase. The aforementioned criterion can be derived independently from the singularity of the staggered susceptibility.[19] It has to be emphasized that Eq. (20) is an essential feature of all HF theories and is quite insensitive to the choice of a more-sophisticated magnetic-interaction term [Eq. (7)] being possibly better adapted to the lattice structure of the fcc lattice.

In the case of alternant lattices and a half-filled band, the right-hand side of the corresponding inequality becomes infinite, the consequence being that the system is conducting only for $U = 0$ and insulating and antiferromagnetic for any nonzero U. In the case of the fcc lattice, the right-hand side of Eq. (20)

proves to be finite for any $\bar{\mu}$ and thus there exists a critical value $U>0$ for the onset of antiferromagnetism for any n_e, $0 \leq n_e \leq 2$. This can be seen when performing two integrations on the right-hand side of Eq. (20). Representative for the whole range of possible values of the chemical potential we only quote the result for $-1 \leq \bar{\mu} \leq 0$, $\bar{\mu}$ and U measured in units of $4J$:

$$U^{-1}=\frac{2}{\pi^3}\int_{(1+\bar{\mu})/2}^{1} dx \ln\left[\frac{1+(1-x^2)^{1/2}}{|x|}\right]K(\bar{k})/(x^2-\bar{\mu})^{1/2}+\frac{8}{\pi^3}\int_{0}^{(1+\bar{\mu})/2} dx \ln\left[\frac{1+(1-x^2)^{1/2}}{|x|}\right]K(k)/(1-\bar{\mu}) \ . \tag{21}$$

K is the complete elliptic integral of the second kind, and the moduli k, $\bar{k}$ are defined by

$$k^2=[(1+\bar{\mu})^2-4x^2]/(1-\bar{\mu})^2$$

and

$$\bar{k}^2=[x^2-\tfrac{1}{4}(1+\bar{\mu})^2]/(x^2-\bar{\mu}) \ .$$

For the remaining values of $\bar{\mu}$ the corresponding formulae are of the same structure and we can immediately deduce that the right-hand side of Eq. (20) converges on the whole interval $-1 \leq \bar{\mu} \leq 3$ which exhausts all possible values of the electron density n_e. The resulting $U_c(\bar{\mu})$ curve is shown in Fig. 2 as line *a*. Having constructed this line in a phase diagram, it is necessary to check whether this onset of antiferromagnetism has a real physical meaning. The authors[13] have already encountered a problem of this kind in the case of the linear Hubbard chain with a nonsymmetric band structure. HF calculations in this simplified model indicate the possibility of a gap collapse. This transition is apparently of first order and the critical value at which the transition takes place is smaller than the value U_c which belongs to the second order transition. In order to investigate the possibility of a gap collapse and to determine the order of the actual transition in the fcc lattice, we have to compute explicitly the gap parameter Δ and the ground-state energy as functions of the interaction strength U.

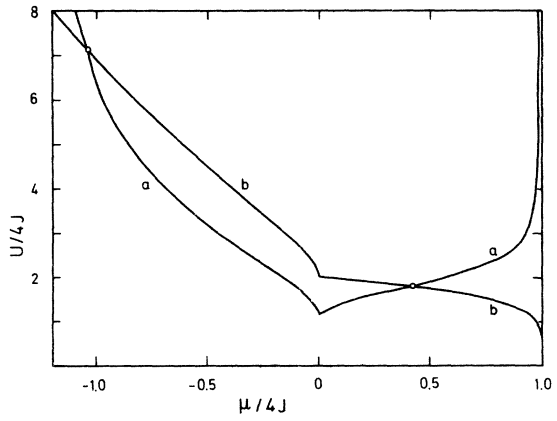

FIG. 2. Second-order phase boundaries above which the antiferromagnetic state (line *a*) and the ferromagnetic state (line *b*) are stable against the paramagnetic phase.

We postpone this numerical treatment and first discuss spin and particle susceptibilities $\chi_s \propto ds_z/d\zeta$ and $\chi_p \propto dn_e/d\mu$. Both represent second derivatives of the thermodynamic potential and are known to be sensitive indicators of phase transitions in a physical system. The second quantity is connected with the electric behavior of the system which means it is porportional to the conductivity. By implicit differentiation of the self-consistency equations one obtains

$$\frac{ds_z}{d\zeta}=\frac{\chi_0}{2-U\chi_0} \tag{22}$$

and

$$\frac{dn_e}{d\mu}=\frac{2G(\bar{\mu})}{2+UG(\bar{\mu})} \ . \tag{23}$$

Here we have defined

$$\chi_0=\frac{1}{N}\sum_{\vec{k}\nu}\left[(-)^{\nu}\left(\frac{\Delta}{E}\right)^2\frac{f(E_\nu)}{E}-\frac{\partial f(E_\nu)}{\partial E_\nu}\left(\frac{\epsilon^{-}-\bar{\zeta}}{E}\right)^2\right] \ . \tag{24}$$

In this expression it is understood that the quantities E_ν, E, ϵ are functions of $\vec{k}$. $G(\bar{\mu})$ stands for

$$G(\bar{\mu})=N^{-1}\sum_{\vec{k},\nu}(-)\frac{\partial f(E_\nu)}{\partial E_\nu} \ , \tag{25}$$

which reduces to the density of states of the two-band system at $T=0$. In this connection, it is interesting to note that χ_0 is the tight-binding analog of a susceptibility used by Fedders and Martin in a paper about itinerant antiferromagnetism.[20]

The denominator in Eq. (23) reflects the explicit dependence of n_e on the effective potential $\bar{\mu}$ and plays a minor role. It cannot cause a singularity in χ_p because the function $G(\bar{\mu})$ is always positive. On the other hand the negative sign in the denominator of Eq. (22) is responsible for the singularity at $U^{-1}=g(\bar{\mu})$ in the paramagnetic (PM) phase at absolute zero indicating the onset of ferromagnetism (Stoner criterion). Here $g(\epsilon)$ is the density of states[17] belonging to the band energy $\epsilon(\vec{k})$ in Eq. (2).

Some additional remarks to Eq. (23) are necessary. Standard procedures in transport theory[21] lead to the conductivity

$$\sigma \propto \frac{1}{N}\sum_{\vec{k},\nu}\left[(-)\frac{\partial f(E_\nu)}{\partial E_\nu}\tau(E_\nu)\frac{1}{3}\left(\frac{\partial E_\nu}{\partial \vec{k}}\right)^2\right] , \quad (26)$$

where some scattering mechanism described by an energy-dependent relaxation time has been assumed. In order to treat the problem exactly one has to know $\tau(E)$ and to evaluate the function[22]

$$v^2(E) = N^{-1}\sum_{\vec{k},\nu}\delta(E - E_\nu(\vec{k}))\frac{1}{3}\left(\frac{\partial E_\nu(\vec{k})}{\partial \vec{k}}\right)^2 , \quad (27)$$

being obviously smoother than the density of states because no Van Hove singularities arise. This suggests a simplifying approximation. We take $\tau(E)$ and $v^2(E)$ out of the sum over k as an averaged quantity denoted by $\langle \tau v^2 \rangle_{av}$ and the conductivity assumes the simple form $\sigma \propto \langle \tau v^2 \rangle_{av} dn_e/d\bar{\mu}$, where the particle susceptibility belonging to the effective chemical potential $\bar{\mu}$ has been used. Calculating this quantity at absolute zero yields

$$\frac{dn_e}{d\bar{\mu}} = N^{-1}\sum_{\vec{k},\nu}\delta(E_\nu(\vec{k})) . \quad (28)$$

This is the density of states of the two-band system. In order to decide whether or not the system is conducting it is sufficient to investigate Eq. (23). It provides as well as Eq. (26) information about the conducting properties within the scope of our approximation and can be obtained simply as the second derivative of the great thermodynamic potential with respect to μ from Eq. (14). In Sec. IV the numerical results are presented.

IV. NUMERICAL RESULTS AND DISCUSSION

The computation of the AFM ground-state energy given by Eq. (16) requires a numerical solution of the two simultaneous equations (17) and (18) which specify the order parameter Δ and the chemical potential μ for fixed values of n_e and U, respectively. In Fig. 3 the gap parameter as a function of U is depicted only in the representative case of a half-filled band, since for all values of n_e, the $\Delta(U)$ curves exhibit the same characteristic shape. We find that a nonzero gap appears first at a certain critical value of the interaction strength U_c^{II}. Note that this quantity is identical with the solution of Eq. (20) where the equality sign holds. Thus the zero of the $\Delta(U)$ curve corresponds to a point of the second-order phase boundary marked as line a in Fig. 2. But the initial increase of the gap with a negative derivative indicates that the physical system will not undergo a second-order phase transition but continues to maintain the AFM ordering as the interaction strength decreases beyond U_c^{II}. Accordingly the PM phase sets in discontinuously at a smaller value of U.

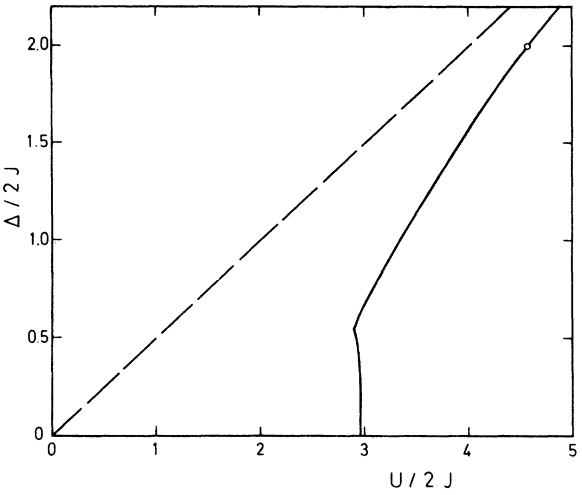

FIG. 3. Gap parameter Δ plotted vs the interaction strength U, both in units of $2J$ in the case $n = 1$. The point marked as a circle indicates the metal-insulator (M-I) transition at $\Delta_{M-I} = 4J$ above which $\Delta \to \frac{1}{2}U$ for large U (dashed line).

In order to locate this critical U_c^I where the superscript I now indicates a transition of first order, we use a well-known procedure which amounts to a comparison of energies in different phases but which requires ultimately knowledge of $\Delta(U)$ only. We suppose that the occurence of a negative $d\Delta/dU$ and the sharp bend in the profile of $\Delta(U)$, which is found to occur at $\Delta = \bar{\mu}$, result from the implicit assumption that the system is homogeneous and the possibility of a coexistence of two phases has not been considered. This suggests performing a Maxwell construction, quite in accordance with the situation in the Vander Waals gas.

As a first step we define the extensive quantity $c = N^{-1}\sum_i \langle n_{i\uparrow} n_{i\downarrow} \rangle$, which measures the concentration of doubly occupied sites and is thermodynamically conjugated to the interaction constant U. Exploiting the gap equation (17), the averaged quantity defining c is readily calculated to give the equation of state

$$c = \frac{1}{N}\sum_i \langle n_{i\uparrow} n_{i\downarrow} \rangle = \frac{n_e^2}{4} - \frac{\Delta^2}{U^2} - s_z^2 . \quad (29)$$

Further, we introduce the Legendre-transformated ground-state energy

$$G(c) = E_0/N - Uc , \quad (30)$$

which depends explicitly on the particlelike quantities n_e, s_z, and c. From this one immediately obtains the Maxwell relation $U = -\partial G/\partial c$. The necessary condition for the two phases to be in equilibrium is the equality of the internal energies $E_0(U)/N$ and of the

intensive variable U. We thus obtain the equilibrium condition which reads in terms of the function G,

$$G_1 - G_2 = U_c^{\mathrm{I}}(c_2 - c_1) \ , \tag{31}$$

which becomes, through use of the Maxwell relation mentioned above,

$$\int_1^2 dc \ U(c) = U_c^{\mathrm{I}}(c_2 - c_1) \ . \tag{32}$$

Thus it is shown that the equal area construction known as Maxwell's rule is a convenient procedure to localize, in a diagram of conjugated variables, the phase transition of first order. At this point, two remarks have to be made. First, it should be noted that the above considerations apply also, with Δ set equal to zero, to the ferromagnetic case $s_z \neq 0$, which will be dealt with at the end of this section. Second, it is to be emphasized that, in making the Maxwell construction, it was necessary to use portions of the $\Delta(U)$ curve we declared to be unphysical. Now we are able to show that these portions represent regions of negative "compressibility" for $d\Delta/dU < 0$ is equivalent to $dc/dU > 0$ due to Eq. (29) and this describes the unphysical state where the number of doubly occupied sites diminishes with decreasing interaction strength U.

Let us now focus our attention again on the AFM case in a half-filled band. The Maxwell construction yields the numerical value $U_c^{\mathrm{I}} = 5.9J$ of the critical interaction strength which is only slightly smaller than the second-order value U_c^{II}. As mentioned above, the calculations of the gap Δ requires a simultaneous determination of the chemical potential $\bar{\mu}$. Thus it is obvious to discuss both quantities together. In the paramagnetic state ($\Delta = 0$), the chemical potential is found to be constant and assumes the numerical value $\bar{\mu}/2J = 0.46$ as shown in Fig. 4. As soon as U reaches the region of two coexisting phases, the function $\bar{\mu}(U)$ is expected to display the same unphysical behavior as $\Delta(U)$. Therefore, depicting $\bar{\mu}(U)$ in Fig. 4, we have already used the result of the Maxwell construction, and, thus, the discontinuous jump of $\bar{\mu}$ occurs at the critical U_c^{I} at which the gap suffers a collapse. The discontinuous bandsplitting, a decreasing of band overlap with increasing U and, finally, a complete band separation govern the further behavior of $\bar{\mu}$. We notice that for values greater than the critical U which indicates the total separation of bands, the chemical potential is found to be identically zero quite in accordance with the behavior of $\bar{\mu}$ in the sc lattice where the magnetic and the metal-insulator transitions are shown to merge at $U = 0$.

With known values of Δ and $\bar{\mu}$ the ground-state energy E_0 is easily calculated. The resulting $E_0(U)$ curve is shown in Fig. 5. The critical point where the AFM ground state leaves the PM line, is marked by a circle. It should be noted that the discontinuity of the derivative of $E_0(U)$ at U_c^{I} is so weak, that a look at the profile of $E_0(U)$ in Fig. 5 cannot yield any information about the order of the phase transition.

In view of the fact that the actual magnetic transition is found to be of first order, line a in Fig. 2 seems to be no reliable phase boundary any longer. But the situation at $n_e = 1$ described above indicates that the exact first-order phase transition nearly coincides with the irrelevant second-order transition. The determination of the exact line over the whole range $-3 \leq \bar{\mu} \leq 1$ is laborious and tedious, because each point requires an equal area construction. Carrying out this procedure at some representative values of $\bar{\mu}$ finally yields the result that indeed the two curves nearly merge. This fact recovers the relevance of line a and justifies the use of second-order boundaries also

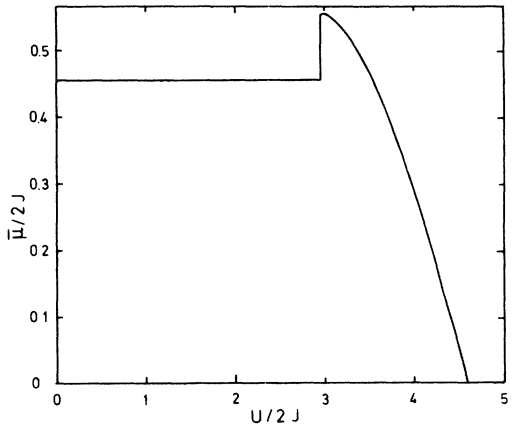

FIG. 4. Chemical potential $\bar{\mu} = \mu - \frac{1}{2}U$ in units of $2J$ plotted against the interaction strength $U/2J$ for $n_e = 1$. The discontinuity at $U/2J = 2.95$ indicates a first-order phase transition and is a result of a Maxwell construction.

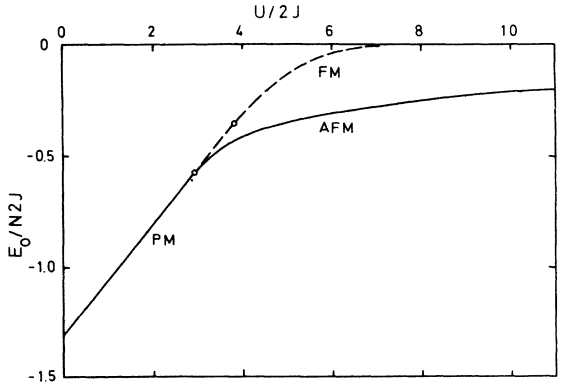

FIG. 5. Ground-state energy per lattice site $E_0/N2J$ in the AFM case (solid line) at $n_e = 1$ compared to the FM case (broken line), both plotted against $U/2J$. Line PM indicates the paramagnetic state and the points marked by circles indicate the phase transitions of first order.

in order to investigate the possible appearance of ferromagnetism.

Before embarking on this program, some remarks concerning the shape of line a have to be made. In contrast to the analogous phase diagrams in AB lattices, given by Penn[5] and Florencio and Chao,[23] the diagram at hand is not symmetric due to the band energies of Eq. (2) and the resulting nonsymmetric density of states. The line a exhibits a peak at $\bar{\mu}=0$. This is a feature being common to the sc and fcc lattice, the only difference being that in the alternant lattice this peak is more pronounced and reaches the abscissa due to the coincidence of the Fermi surface and the magnetic phase boundary for a band occupation $n_e=1$.[5] This coincidence which results in a singularity of the right-hand side of inequality (20) is destroyed as soon as NNN hopping has been taken into account in an AB lattice or the band structure becomes nonsymmetric as in the case of the fcc lattice. The rudimentary spike in the present phase diagram appears, like its analog in an AB lattice, at the surface $\epsilon(k)=\bar{\mu}=0$ but the corresponding electron density is now $n_e=0.78$. The nonvanishing minimum value of U_c at the peak of the phase boundary a reflects the property of the fcc lattice that the onset of AF ordering needs a finite coupling constant for any value of n_e.

At $\bar{\mu}=+1$ and $\bar{\mu}=-3$ the critical U tends to infinity which can easily be seen from Eq. (20),

$$U_c^{-1}=\int_{-1}^{1}dx\int_{-2}^{2}dy\,\frac{\Theta(\bar{\mu}-x+y)g(x,y)}{y}\ , \qquad (33)$$

expressed in terms of the combined density of states [Eq. (15)]. In the first case the step function Θ causes no restriction for the integration, and symmetry considerations yield a vanishing integral; in the second case the integrand of Eq. (33) is identically zero.

Let us now discuss the second line b in Fig. 2. It is the phase boundary between a ferromagnetic and paramagnetic phase, and has been calculated using the Stoner criterion

$$U^{\mathrm{FM}}(\bar{\mu})=1/g(\bar{\mu})\ . \qquad (34)$$

Of course, the use of this criterion implies that the resulting line b is a second-order phase boundary. But, looking at Fig. 6 which represents the magnetization s_z as a function of U in the case of a half-filled band, we recognize that the magnetic transition is apparently of first order because of the collapse of the order parameter. Investigating the magnetization for electron densities $n_e\neq 1$, one finds the same situation. This means the system itself realizes a Maxwell construction and the ferromagnetic phase sets in discontinuously at a critical U defined by Eq. (34).

Bearing in mind that both lines in Fig. 2 must now be reinterpreted as phase boundaries of first order, one might expect from the phase diagram that in the

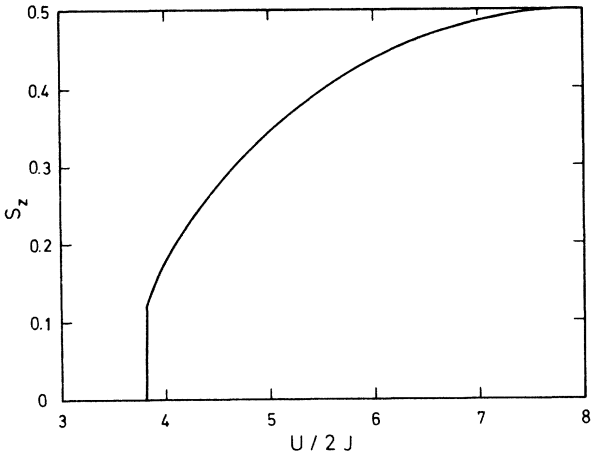

FIG. 6. Magnetization per lattice site s_z vs the interaction strength $U/2J$ in the case $n_e=1$.

region $-1.04\leq\bar{\mu}/4J\leq 0.42$, among the possible magnetic states, the ferromagnetic one is never the state of lowest energy. We test this assumption by an actual energy comparison. This has been displayed in the representative case of a half-filled band in Fig. 5, revealing unambiguously the AFM phase to be the stable one. This situation is found throughout the interval of $\bar{\mu}$, where the AFM line lies markedly below the FM line b, unless the repulsive potential U becomes very large. The extreme strong-coupling limit requires a special investigation. A discussion of how the stability criterion must be modified is given in Appendix B. There it is shown that in the particular case of an almost half-filled band our simple model exhibits ferromagnetism for $n_e>1$ and a ground state which is no longer ferromagnetic as soon as $n_e\leq 1$ completely in accord with the predictions of Nagaoka's rigorous investigations in the limiting case $U\rightarrow\infty$.[24]

The two magnetic phase boundaries cross each other at $\bar{\mu}/4J=-1.04$ and $\bar{\mu}/4J=0.42$ belonging to the electron density $n_e=0.27$ and $n_e=1.21$, respectively. In the vicinity of these intersection points a very accurate calculation of the corresponding ground-state energies has to be performed in order to decide which kind of magnetism is favored. This possibly reveals additional magnetic transitions. But in the limiting cases of a nearly empty or nearly full band we can immediately deduce, without a comparison of energies, that line a, representing the onset of AFM, becomes meaningless. In the case of a nearly filled band ($n_e\rightarrow 2$), it is seen that the additional energy which has to be afforded in order to establish the ferromagnetic (FM) state, is overcompensated by the reduction of repulsive energy between opposite spins, entailing the stability of the FM phase against AFM and PM beyond line b. Finally, when the band is almost empty, we see that only the paramagnetic state exists for

not too large values of $U/2J$.

In Fig. 7 the particle susceptibility $dn_e/d\mu$ is shown as a function of $U/2J$. As has been discussed above this quantity describes the electric behavior of our system. Three successive regions are obtained: A metallic one combined with paramagnetism, an antiferromagnetic metal—which could be better called a semimetal, because this second phase is characterized by band overlapping—and finally with further increasing U an antiferromagnetic insulator. The discontinuity at U_c^1 of the order parameter Δ entails a jump in the particle susceptibility and decreases abruptly the conductivity. The successive semimetal region is characterized by both bands being partially occupied. Clearly, turning on the "magnetic field" Δ lifts the twofold spin degeneracy.

Due to Eq. (12), there exist for each k vector two energy values separated by at least 2Δ. But despite this gap, in certain regions of the Brillouin zone a shift from one band to the other is possible with an appropriate translation vector $\vec{Q}$ depending on $\vec{k}$ and satisfying the equation $E_1(\vec{k}) = E_2(\vec{k}+\vec{Q})$. This allowed band-changing at the same energy value just represents the mechanism which is responsible for retaining metallic properties. In order to account for the decreasing of the conductivity with increasing $U > U_c^1$ we want to make the point, that the analog to the metallic Fermi surface $\epsilon(\vec{k}) - \bar{\mu} = 0$ is now the two surfaces in the Brillouin zone defined by $E_1(\vec{k}) = 0$, $E_2(\vec{k}) = 0$. Obviously these regions are smaller than the Fermi surface available for conductivity in the metallic paramagnetic state. They diminish with increasing Δ and vanish at U_{M-I} (M-I denotes the metal-insulator transition) where band-separation produces an insulating phase, and $dn_e/d\mu$ falls off to zero.

To understand this transition to a totally insulating AFM phase, we consider the band structure $E_{1,2}(\vec{k})$ of Eq. (12) again. The condition that the bands cease to overlap may be expressed by the equation

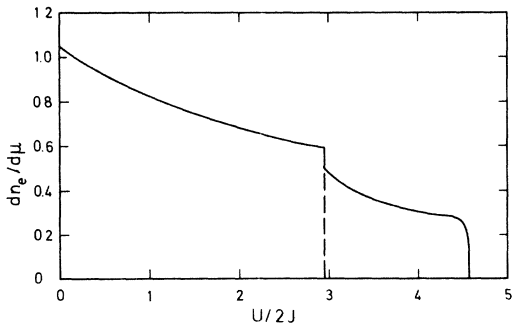

FIG. 7. Particle susceptibility describing the conducting properties in the PM phase ($U/2J < 2.95$) and the AFM phase ($U/2J > 2.95$) for a half-filled band. The zero at $U/2J = 4.56$ corresponds to the gap parameter $\Delta_{M-I} = 4J$.

$E_{1\,\min} = E_{2\,\max}$, where $E_{1\,\min}$ denotes the bottom of the upper and $E_{2\,\max}$ the top of the lower band. The calculation of this condition is elementary. Using the inequalities $-4J \leq \epsilon^+(\vec{k}) \leq 4J$ the band-edge energies are easily determined to be $E_{1\,\min} = -4J + \Delta$ $E_{2\,\max} = 4J - \Delta$. Equating these values yields for the critical gap parameter the result $\Delta_{M-I} = 4J$. The gap equation (17) determines the corresponding critical value U_{M-I}. A numerical calculation yields $U_{M-I}/2J = 4.56$.

The second response function of interest, the magnetic susceptibility χ_s, is shown in Fig. 8 in the case of a half-filled band and for $\zeta = 0$. In the paramagnetic phase ($\Delta = 0$), this quantity, defined by Eq. (22), reduces to $g(\bar{\mu})/[1 - Ug(\bar{\mu})]$. The numerator, representing the Pauli paramagnetism, measures the density of states at the Fermi level and is thus independent of the interaction strength U. Therefore, the shape of χ_s in the PM phase is governed by the singularity at $U = 1/g(\bar{\mu})$. We recall that this equation is the standard condition for ferromagnetism used in order to establish line b in the phase diagram in Fig. 2. But the ferromagnetic phase boundary b has been found to be meaningless at $n_e \approx 1$, and consequently the onset of AFM at the critical U_c^1 prevents the susceptibility from diverging.

Quite analogously to the particle susceptibility, the abrupt appearance of a finite-order parameter Δ at the phase transition gives rise to a jump of χ_s at U_c^1. In order to understand in more physical terms why the polarizability increases discontinuously, we first note that it is sufficient to investigate the behavior of the quantity χ_0 given by Eq. (24). Indeed, the denominator $(2 - U\chi_0)$ in Eq. (22), defining χ_s, has only the effect of amplifying tendencies to rise or to fall. As a

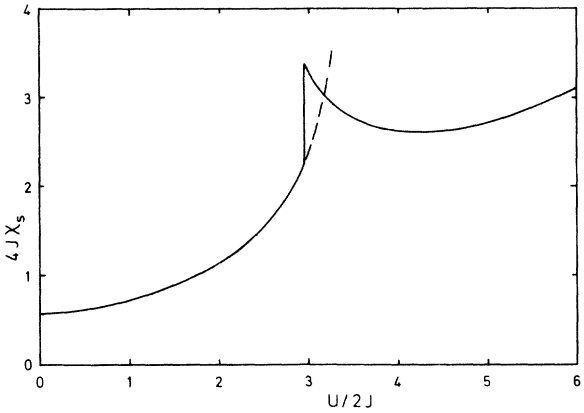

FIG. 8. Susceptibility in units of $1/4J$ as a function of $U/2J$ for $n_e = 1$. The continuation (broken line) of the paramagnetic susceptibility into the region of AFM assumes an infinite value at $U/2J = 3.8$ which determines a corresponding point of the ferromagnetic phase boundary in Fig. 2.

next step we express χ_0 in the more tangible form

$$\chi_0 = G(\bar{\mu}) + 2\Delta U^{-2} \frac{\partial U(\Delta)}{\partial \Delta} , \tag{35}$$

where the gap equation (17) and Eq. (25) have been used. The first term in Eq. (35) is directly related to the conduction properties by virtue of Eq. (23) and suffers an abrupt decreasing at U_c^1, as has been discussed already. The second competitive term is determined by the shape of the known $\Delta(U)$ curve, displayed in Fig. 3 and is easily found to be positive in the whole region $U > U_c^1$. Thus, turning on the order parameter Δ at a finite value entails a jump of the second term which is markedly stronger than the weak discontinuity of $G(\bar{\mu})$.

At first sight, an abrupt increasing of $\chi_\perp$ at the onset of AFM seems to be a quite peculiar behavior. But it has to be emphasized that $\chi_\perp$ represents a perpendicular susceptibility. Then the peak at U_c^1 indicates that an existing AFM ordering favors the alignment of spins in a direction, perpendicular to the AFM order.

As soon as the two bands are totally separated, only the second term in Eq. (35) survives. For still larger values of U, the system degenerates to completely localized spins and Δ behaves roughly like $\frac{1}{2}U$ entailing the asymptotic behavior $\chi_s^{-1} \sim 2\Delta - U$ which accounts for the rise and the divergence of χ_s at $U \to \infty$.

V. CONCLUSION

We have considered the onset of antiferromagnetism in the Hubbard model for a nonalternant lattice using the HFA. At 0 °K, we find the following three phases of the system with increasing U: (i) paramagnetic metal, (ii) noninsulating antiferromagnet, and (iii) antiferromagnetic insulator, provided the band is half-filled.

The appearance of these successive phases contrasts with results of the HF treatment for an alternant lattice where only the AFM insulator phase occurs, and moreover invalidates the notion that in the paramagnetic phase the HFA disregards the tendency of opposite spin electrons to avoid double occupations and hence produces AFM ordering too easily. We believe that the suppression of the paramagnetic metallic phase in alternant lattices is a feature inherent in the model rather than a consequence of a rough approximation. The reason is that the onset of AFM at $U = 0$ in AB lattices for $n_e = 1$ is unequivocally associated with the coincidence of the magnetic zone boundary and the Fermi surface, which must be destroyed in order to remove the onset of AFM to a nonzero value of U. This distortion can be accomplished when adding or extracting one electron,[5] or turning on NNN hopping[13] or choosing a lattice with a nonsymmetric band structure as has been done in this paper.

In the case of one electron per atom the AFM phase has been carefully investigated. The magnetic transition into the AFM order occurs at a critical $U_c^1/J = 5.9$ and is combined with a discontinuous decrease of conductivity. This proves to be quite in accordance with Slater,[25] who first introduced the idea that the AFM order may cause a splitting of the band, degrading the metallic properties. In contrast to AB lattices, the magnetic transition does not coincide with the *M-I* transition but this transition from an AFM metal to an AFM insulator now occurs on increasing U and appears as a band-crossing transition.

Comparison of these HF results with experimental data of transition-metal oxides has to be done at the absolute zero of temperature, where transitions of those materials can occur only under pressure or with varying composition. This means a confirmation of the present results requires materials with a lattice constant a that can be varied, and moreover requires the experimental results to be extrapolated smoothly to $T = 0$. Keeping in mind that the dependence of the hopping strength J on a is given by $J = \hbar^2/2ma^2$ and that the physical quantities in the present model are given as functions of the Coulomb repulsion U in units of J, we find that a decrease of U can be brought about by reducing the lattice constant a.

Measurements on pure and doped V_2O_3 at low temperature indicate that a pressure-induced transition occurs between a high-pressure metallic state and a lower-pressure antiferromagnetic-insulating state.[26] Moreover, electrical resistivity and magnetic susceptibility as functions of pressure exhibit all the qualitative features found in the present model.[27-29]

A complete consistency with available experimental results cannot be expected in view of the facts that the Hubbard Hamiltonian only allows the description of narrow s bands and that the fcc lattice investigated in this paper is by no means the lattice type appropriate for the description of a system as complicated as V_2O_3. It is for this reason that the model used in this paper cannot be expected to give a V_2O_3-type phase diagram, for example. At any rate, the calculation of phase boundaries confirms once more how cautiously one has to handle phase transitions. The second-order phase boundaries in Fig. 2 have been found by a method which is equivalent to a response function technique. But investigations of the energetic stability of the magnetic ordered states revealed those lines to be of no physical significance and required a Maxwell construction. The resulting phase boundaries indicate first-order transitions but happen to coincide nearly with the old ones. Nevertheless, this circumstance may serve as a warning when using the response function method to construct phase diagrams. This method analyses only stability against infinitesimal external perturbations which is misleading in the case at hand, where the phase transition occurs while the state is still stable against infinitesimal perturbations.

Moreover, it should be pointed out that due to the

present results one is forced to lay emphasis, in the future, on the exact evaluation of the summations over the Brillouin zone which are involved in the equations. Simulating the properties of various lattice types by simply changing the coordination number, as Florencio and Chao[23] did, appears to be insufficient. Also the "parabolic density of states," introduced for the first time by Hubbard[1] and then frequently used by other authors owing ot its simplicity, would have been too crude an approximation to make the present results available.

APPENDIX A

For numerical purpose we define the combined density of states

$$g(x,y)=N^{-1}\sum_{\vec{k}}\delta(x-\epsilon^{+}(\vec{k}))\delta(y-\epsilon^{-}(\vec{k}))\ . \tag{A1}$$

Expressing the sum over allowed k vectors of the Brillouin zone as an integral, we obtain after some elementary transformations

$$\tilde{g}=\int_{-1}^{1}\int_{-1}^{1}\int\prod_{j=1}^{3}dl_j(1-l_j^2)^{-1/2}\delta(x+l_1l_2)\times\delta(y+l_2l_3+l_3l_1)\ , \tag{A2}$$

where x,y are now dimensionless quantities measured in units of $4J$, and $\tilde{g}$ stands for $g\pi^3(4J)^2$.

We perform the integration over l_3 and get

$$\tilde{g}=\int\int_{\mathrm{I+II}}\prod_{j=1}^{2}dl_j(1-l_j^2)^{-1/2}\delta(x+l_1l_2)\times[(l_1+l_2)^2-y^2]^{-1/2}\ , \tag{A3}$$

where the domains of integration I,II are determined by $|y|\leq|l_1+l_2|$. For reasons of symmetry, the integration may be restricted to one of the two domains, say I. There is another simplification arising from the fact, that g is an even function of y. Thus we can confine ourselves to the case $y>0$. Performing the integration over l_2 and utilizing the remaining δ function $\delta(x+l_1l_2)$ finally yields

$$\tilde{g}=2\int_{-1+y}^{1}dl_1\frac{J(l_1)}{(1-l_1^2)^{1/2}}\ , \tag{A4}$$

where J is defined by

$$J(l_1)=\begin{cases}(l_1^2-x^2)^{-1/2}\{[(l_1^2-x)/l_1]^2-y^2\}^{-1/2} & \text{for } y-l_1\leq -x/l_1\leq 1\ ,\\ 0 & \text{otherwise}\ .\end{cases} \tag{A5}$$

We now have to distinguish the two cases $x+\frac{1}{4}y^2\lesseqgtr 0$. Finally, $\tilde{g}$ can be expressed in terms of the first complete elliptic integral

$$\tilde{g}=\begin{cases}2K(k)[2kk'/s(1-x^2)]^{1/2} & \text{for } x+\frac{1}{4}y^2<0\ ,\\ 4K(\bar{k})/[(1-y_-^2)(y_+^2-x^2)]^{1/2} & \text{for } x+\frac{1}{4}y^2>0\ ,\end{cases} \tag{A6}$$

where

$$k^2=1-k'^2=\tfrac{1}{2}\{1-[s^2+(1-r)(x^2-r)]\times[s^2+(1-r)^2]^{-1/2}\times[s^2+(x^2-r)^2]^{-1/2}\}\ , \tag{A7}$$

$$r=x+\tfrac{1}{2}y^2\ , \tag{A8}$$

$$s=y(|x|-\tfrac{1}{4}y^2)^{1/2}\ , \tag{A9}$$

$$y_\pm=\tfrac{1}{2}y\pm(x+\tfrac{1}{4}y^2)^{1/2}\ , \tag{A10}$$

$$\bar{k}^2=(1-y_+^2)(y_-^2-x^2)/(1-y_-^2)(y_+^2-x^2) \tag{A11}$$

APPENDIX B

Here we show that the approximate results of the present paper coincide with the exact results of Nagaoka[24] in the strong-coupling limit. To this end we investigate Eqs. (16)–(19) for $U\to\infty$ and compare the asymptotic forms of the ground state energies of the two competing magnetic states. As a first step we study the AFM state and confine ourselves to the case of an almost half-filled band $|1-n_e|\ll 1$. Here the gap equation (17) is given by

$$\frac{2}{U}=\frac{1}{N}\sum_{\vec{k}}\frac{1}{E(\vec{k})}-\frac{|1-n_e|}{\Delta}\ , \tag{B1}$$

and thus the gap varies as $\frac{1}{2}(1-|1-n_e|)U$ for $U\to\infty$. With this limiting behavior of Δ the AFM ground-state energy is easily determined as

$$\frac{E_0}{N}\sim\begin{cases}(n_e-1)(\epsilon_{\min}^{+}+U) & \text{for } n_e>1\ .\\ (n_e-1)\epsilon_{\max}^{+} & \text{for } n_e<1\ .\end{cases} \tag{B2}$$

The ferromagnetic state and the determination of the

asymptotic form of the energy per lattice point requires the solution of Eq. (19) instead of the gap equation. In the ferromagnetic case Eq. (19) reduces to

$$4s_z = \frac{1}{N}\sum_{\vec{k}} \{\mathrm{sgn}\,[\epsilon(\vec{k}) - \bar{\mu} + Us_z] - \mathrm{sgn}[\epsilon(\vec{k}) - \bar{\mu} - Us_z]\} \tag{B3}$$

This relation, together with the Eq. (18), implies that the maximum possible magnetization for a given n_e is

$$s_z^{\max} = \tfrac{1}{2}(1 - |1 - n_e|) \ . \tag{B4}$$

From Eq. (16) it follows that the maximally magnetized ground-state energy is

$$\frac{E_0}{N} \sim \begin{cases} (n_e - 1)(U + \epsilon_{\min}) & \text{for } n_e > 1 \ , \\ (n_e - 1)\epsilon_{\max} & \text{for } n_e < 1 \ . \end{cases} \tag{B5}$$

We have summarized the information contained in Eqs. (B2) and (B5) in Table I. This table indicates the state of lowest energy among the ferromagnetic and antiferromagnetic states in the strong-coupling limit ($U \to \infty$) depending on the sign of $n_e - 1$. Bearing in mind that in the fcc lattice $\epsilon_{\max} = \epsilon^+_{\max} = 4J$ and $\epsilon_{\min} = -12J < \epsilon^+_{\min} = -4J$, and comparing the energies of the various magnetic states, it is found that the ferromagnetic state with maximum total spin is not the ground state, if $n_e \leq 1$, and the ferromagnetic ordering with $s_z = s_z^{\max}$ is favored, if $n_e > 1$. Thus the HF results in this paper are consistent with the predictions of Nagaoka[24] who studied the role of holes and excess electrons quite rigorously in an almost half-filled band with a strong repulsive Coulomb interaction.

TABLE I. Summary of the information contained in Eqs. (B2) and (B5).

	FM	AFM
$n_e > 1$	$(n_e - 1)(U + \epsilon_{\min})$	$(n_e - 1)(U + \epsilon^+_{\min})$
$n_e < 1$	$-(1 - n_e)\epsilon_{\max}$	$-(1 - n_e)\epsilon^+_{\max}$

*Permanent address: Max-Planck-Institut für Physik und Astrophysik, Institut für Extraterrestrische Physik, Garching, bei München, West Germany.

[1]J. Hubbard, Proc. R. Soc. A 276, 238 (1963); 281, 401 (1964).
[2]W. F. Brinkman and T. M. Rice, Phys. Rev. B 2, 1324 (1970).
[3]L. G. Caron and G. Kemeny, Phys. Rev. B 3, 3007 (1971).
[4]J. des Cloizeaux, J. Phys. Radium 20, 606 (1959); 20, 751 (1959).
[5]D. Penn, Phys. Rev. 142, 350 (1966).
[6]M. Morris and J. Cornwell, J. Phys. C 1, 1145 (1968).
[7]W. Langer, M. Plischke, and D. Mattis, Phys. Rev. Lett. 23, 1448 (1969).
[8]M. Cyrot, Philos. Mag. 25, 1031 (1972).
[9]K. Dichtel, R. J. Jelitto, and H. Koppe, Z. Phys. 246, 248 (1971).
[10]U. Brandt, Z. Phys. 257, 320 (1972).
[11]E. Lieb and F. Wu, Phys. Rev. Lett. 20, 1445 (1968).
[12]B. Brandow, J. Phys. C 8, L357 (1975).
[13]E. Marsch, W. -H. Steeb, and D. Grensing, J. Phys. F 7, 401 (1977).
[14]A. Panten, Diplomarbeit (Universität Kiel, Kiel, 1973) (unpublished).
[15]A. Fetter and J. Walecka, *Quantum Theory of Many Particle Systems* (McGraw-Hill, New York, 1971).
[16]D. Grensing and H. Koppe, Z. Phys. B 23, 199 (1976).
[17]R. J. Jelitto, J. Phys. Chem. Solids 30, 609 (1969).
[18]M. Heise and R. J. Jelitto, Z. Phys. B 25, 381 (1976).
[19]T. Izuyama, D. J. Kim, and R. Kubo, J. Phys. Soc. Jpn. 18, 1025 (1963).
[20]P. A. Fedders and P. Martin, Phys. Rev. 143, 245 (1966).
[21]W. Jones and N. H. March, *Theoretical Solid State Physics* (Wiley, London, 1973), Vol. I, p. 701.
[22]E. Marsch, Z. Phys. B 25, 83 (1976).
[23]J. Florencio and K. A. Chao, Phys. Rev. B 14, 3121 (1976).
[24]Y. Nagaoka, Phys. Rev. 147, 392 (1966).
[25]J. C. Slater, Phys. Rev. 82, 538 (1951).
[26]D. B. McWhan, A. Menth, J. P. Remeika, W. F. Brinkman, and T. M. Rice Phys. Rev. B 7, 1920 (1973).
[27]D. B. McWhan and J. P. Remeika, Phys. Rev. B 2, 3734 (1970).
[28]A. Jayaraman, D. B. McWhan, J. P. Remeika, and P. D. Dernier, Phys. Rev. B 2, 3751 (1970).
[29]A. Menth and J. P. Remeika, Phys. Rev. B 2, 3756 (1970).